The effect of breathing irregularities on quantitative accuracy of respiratory gated PET/CT

Teo, Boon-Keng; Saboury, Babak; Munbodh, Reshma; Scheuermann, Joshua; Torigian, Drew A; Zaidi, Habib; Alavi, Abass

The effect of breathing irregularities on quantitative accuracy of respiratory gated PET/CT

Boon-Keng Teo[a)]
Department of Radiation Oncology, University of Pennsylvania, Philadelphia, Pennsylvania 19104

Babak Saboury
Department of Radiology, University of Pennsylvania, Philadelphia, Pennsylvania 19104

Reshma Munbodh
Department of Radiation Oncology, University of Pennsylvania, Philadelphia, Pennsylvania 19104

Joshua Scheuermann and Drew A. Torigian
Department of Radiology, University of Pennsylvania, Philadelphia, Pennsylvania 19104

Habib Zaidi
Department of Nuclear Medicine and Molecular Imaging, Geneva University Hospital, CH-1211 Geneva, Switzerland; Geneva Neuroscience Center, Geneva University, CH-1205 Geneva, Switzerland; and Department of Nuclear Medicine and Molecular Imaging, University Medical Center Groningen, University of Groningen, 9700 RB Groningen, Netherlands

Abass Alavi
Department of Radiology, University of Pennsylvania, Philadelphia, Pennsylvania 19104

(Received 17 August 2012; revised 25 October 2012; accepted for publication 25 October 2012; published 27 November 2012)

Purpose: 4D positron emission tomography and computed tomography (PET/CT) can be used to reduce motion artifacts by correlating the raw PET data with the respiratory cycle. The accuracy of each PET phase is dependent on the reproducibility and consistency of the breathing cycle during acquisition. The objective of this study is to evaluate the impact of breathing amplitude and phase irregularities on the quantitative accuracy of 4D PET standardized uptake value (SUV) measurements. In addition, the magnitude of quantitative errors due to respiratory motion and partial volume error are compared.

Methods: Phantom studies were performed using spheres filled with ^{18}F ranging from 9 to 47 mm in diameter with background activity. Motion was simulated using patient breathing data. The authors compared the accuracy of SUVs derived from gated PET (4 bins and 8 bins, phase-based) for ideal, average, and highly irregular breathing patterns.

Results: Under ideal conditions, gated PET produced SUVs that were within $(-5.4 \pm 5.3)\%$ of the static phantom measurements averaged across all sphere sizes. With breathing irregularities, the quantitative accuracy of gated PET decreased. Gated PET SUVs (best of 4 bins) were $(-9.6 \pm 13.0)\%$ of the actual value for an average breather and decreased to $(-17.1 \pm 10.8)\%$ for a highly irregular breather. Without gating, the differences in the SUV from actual value were $(-28.5 \pm 18.2)\%$, $(-25.9 \pm 14.4)\%$, and $(-27.9 \pm 18.2)\%$ for the ideal, average, and highly irregular breather, respectively.

Conclusions: Breathing irregularities reduce the quantitative accuracy of gated PET/CT. Current gated PET techniques may underestimate the actual lesion SUV due to phase assignment errors. Evaluation of respiratory trace is necessary to assess accuracy of data binning and its effect on 4D PET SUVs. © *2012 American Association of Physicists in Medicine*. [http://dx.doi.org/10.1118/1.4766876]

Key words: PET/CT imaging, 4D PET, respiratory motion, quantification, gating

I. INTRODUCTION

Integrated positron emission tomography and computed tomography (PET/CT) systems are widely used in the diagnosis, staging, and treatment of cancer and other disorders.[1,2] Fluorodeoxyglucose (^{18}F)-FDG PET/CT, in particular, is routinely used for delineation of gross tumor volume[3–9] in radiation treatment planning. The standardized uptake value (SUV) of the lesion is the most commonly used parameter to assess tumor biology and evaluation of treatment response. One of the key challenges of this semiquantitative method for imaging thoracic tumors on current PET/CT systems is the effect of respiratory motion.[10,11] The image acquisition time required at each bed position typically ranges from 2 to 4 min. This gives rise to image blurring over multiple respiratory cycles and alters the overall appearance and metabolic measures of disease activity. One way to reduce motion artifacts is through respiratory gating.[12,13] Respiratory gated PET is commonly referred to as 4D PET and is commercially available from all major PET/CT vendors. Studies have shown

that gated PET images can reduce the effect of motion blurring and give rise to higher SUV for the lesions examined. PET images with reduced motion blurring appear sharper and presumably provide reliably accurate measures of tumor metabolism.[14]

Respiratory motion artifacts can be minimized using breath hold techniques[15] or 4D respiratory gating systems.[16] These 4D systems work by correlating PET data acquisition with the breathing phase, enabling multiple PET images of different respiratory phases to be reconstructed as distinct scans. By splitting the raw data into multiple phases or bins, each phase image will, in principle, have reduced motion smearing but a higher level of noise due to the poorer count statistics. The key to a good 4D scan is a highly stable breathing pattern that enables accurate data binning. Amplitude based binning methods[17,18] have been shown to give better results than phase binning in situations when there are breathing period or amplitude variations but is not widely available commercially. Phase binning is particularly prone to respiratory signal baseline drift and amplitude irregularities which lead to binning errors. More advanced sorting techniques based on multiple points have been developed to improve data binning in 4D CT.[19]

Clinical PET imaging systems have limited spatial resolution typically in the range of 5–8 mm. This results in inaccurate quantification of radiotracer concentration in tumors measuring less than twice the spatial resolution of the imaging system.[20] This is known as partial volume effect (PVE), and causes lesions to appear smeared, thereby leading to underestimation of radiotracer uptake and an increase in the apparent size of the object imaged. The combined effects of PVE and motion can, in principle, be corrected if both the tumor size and motion amplitude are known. In most cases, tumor size can be estimated from an anatomical imaging modality such as CT, but measurement of tumor respiratory motion amplitude can potentially be accomplished through gating technology such as 4D CT or other advanced imaging techniques such as dynamic magnetic resonance imaging.

Several methodologies have been developed to correct for PVE in oncological PET imaging.[20] One of the simplest methods consists in the use of a table with precalculated correction factors[21] derived from simulation or phantom measurements for a range of estimated tumor sizes and tumor-to-background ratios. More advanced methods use *a priori* information provided by higher resolution anatomical images such as CT or MRI offered by either stand alone or integrated multimodality imaging systems to correct for the suboptimal spatial resolution of PET.[22] Several authors have developed techniques to correct for PVE using the point spread function information within iterative image reconstruction or by postprocessing of PET images via deconvolution.[23,24]

In this paper, we investigate the combined effects of PVE and breathing irregularities on 4D PET data binning and its impact on the quantitative accuracy of SUVs in 4D PET. In addition, we quantify the impact of respiratory motion on the accuracy of nongated PET SUV estimates as a function of tumor size and motion amplitude.

II. MATERIALS AND METHODS

II.A. Simulation study

In order to estimate the impact of motion blurring on SUV measurements, a mathematical phantom was used to simulate spherical lesions of various diameters (8–48 mm; voxel size $= 1.0 \times 1.0 \times 1.0$ mm^3). Tumor-to-background ratios of 5:1 and 15:1 were simulated. Each sphere was assigned identical activity concentration and convolved with a three-dimensional Gaussian point spread function of 8.0 mm full width half max (FWHM) to simulate PVE. The digital image was further smoothed by a top hat filter to simulate linear motion in one dimension. The recovery coefficient, defined as the maximum measured activity relative to the actual value, was then calculated for a range of motion amplitudes ranging from 5 to 30 mm.

II.B. 4D PET/CT phantom study

Experimental measurements were performed using a 22 cm diameter cylindrical phantom containing six fillable spheres of inner diameters 9, 12, 14, 20, 29, and 47 mm. All spheres were filled with identical activity concentration of 42.2 kBq/cc (SUV $= 15$) of ^{18}F except for the 47 mm sphere which had half of this concentration. The largest sphere had half the concentration in order to reduce the total count rate from the phantom and prevent count rate effects from impacting the image quality. The results for the 47 mm sphere measurements were rescaled accordingly for the analysis. The background was filled with an activity concentration of 2.8 kBq/cc (SUV $= 1$). A programmable respiratory motion platform (Modus Medical Devices Inc., Ontario, Canada) was used to drive the phantom along the scanner axial direction using representative patient respiratory waveforms captured with the real-time position management (RPM) system (Varian Medical Systems, Palo Alto, CA). The RPM system uses a camera based system that records the vertical displacement of the chest wall during respiration. Three motion files representing ideal breathing, average breathing, and highly irregular breathing patterns were used. The motion file representing ideal motion was a sinusoidal waveform generated from software while those for the average (some random variations in phase or amplitude) and highly irregular breather (large variations in phase or amplitude) were actual patient breathing patterns. The PET/CT images were acquired on a Philips Gemini TF Big Bore PET/CT (Philips Healthcare, Andover, MA). The 4D PET/CT protocol consisted of a nongated CT, a 4D CT with 8 gates (retrospective spiral with phase binning) followed by a 4D PET (Varian RPM) acquisition for 6 min in one bed position. Reconstructed PET images (voxel size $= 4 \times 4 \times 4$ mm^3) consisted of a nongated PET and gated 4D PET using 4 gates (phase binning). Attenuation correction was performed using the average CT for the nongated PET and phase matched 4D CT for the 4D PET. An additional 4D PET with 8 gates was reconstructed to study the effects of image noise due to fewer counts per phase bin.

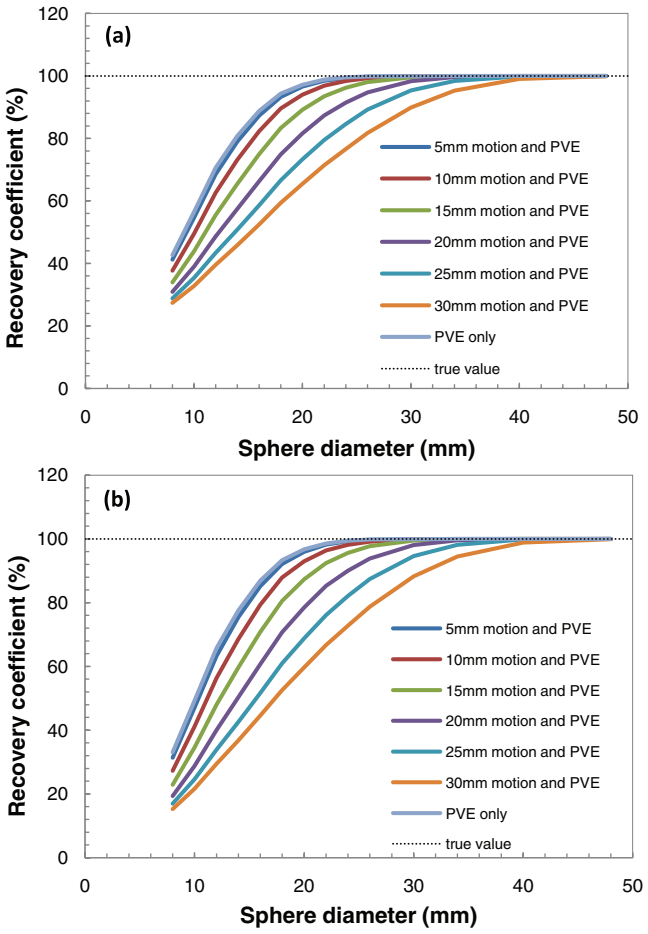

FIG. 1. Simulated effect of motion on tumor SUV including PVE for a 5:1 (a) and 15:1 (b) tumor-to-background ratio.

II.C. Breathing pattern analysis

The respiratory signals acquired by the RPM system were sorted into evenly spaced bins defined from 0% to 100% of the respiratory cycle. A linear relationship between the phantom displacement along the axis of motion and the external respiratory signal was assumed. For each respiratory cycle, the maximum inhale phase was designated as 0% (or 100%), while the maximum exhale is usually close to 50% depending on the breathing pattern. Each bin was labeled using the starting phase of the bin. For example, if four bins are used, the bin width will be 25% and the bin labeled 12.5% will consist of data with phases between 12.5% and 37.5%. Phase sorting accuracy was evaluated by plotting the phantom displacement against the assigned phase for all respiratory cycles. For each bin, the average and standard deviation of the displacement were computed.

II.D. Statistical analysis

SUV_{max} was used for comparison between the gated and nongated PET images. The mean and standard deviations of the SUV_{max} for the 4D PET were determined as a function of sphere diameter for the ideal, average, and highly irregular breathing patterns.

III. RESULTS

III.A. Computer simulation

The simulated effects of partial volume and motion as a function of sphere diameter are presented in Figs. 1(a) and 1(b) for 5:1 and 15:1 tumor-to-background ratios, respectively. All curves exhibit a systematic decrease in recovery coefficient as the sphere diameter decreases owing to PVE. As motion amplitude increases, the measured activity is spread out over a larger volume resulting in a further decrease in apparent SUV_{max}. One salient feature in the figures is that the impact of motion on SUV can be considered small (less than 10%) unless the motion amplitude is comparable to the size of the sphere. The main contribution for the loss in recovery coefficient is from PVE. For a 15:1 tumor-to-background ratio, the additional decrease in recovery coefficients due to motion for the 10, 15, 20, 25, and 30 mm diameter spheres subject to motion equal to its size are 8%, 17%, 18%, 15%, and 12%, respectively.

III.B. Motion evaluation for 4D PET/CT phantom study

The motion file used for the sinusoidal breathing pattern representing ideal breathing with peak to peak motion amplitude of 1.5 cm is presented in Fig. 2(a) together with the phase sorted displacement over the single bed PET acquisition [Fig. 2(b)]. The binned displacement indicates good

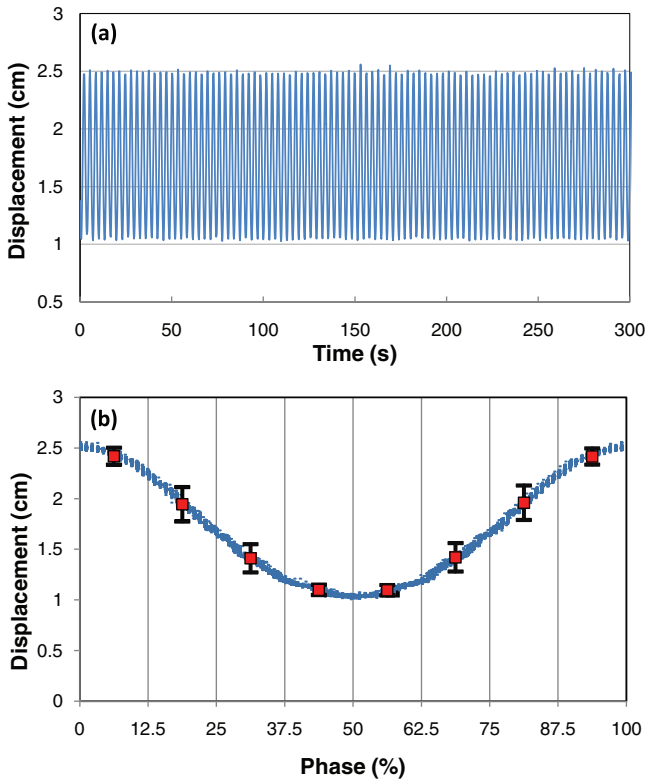

FIG. 2. (a) Phantom motion representing an ideal breather using sinusoidal waveform. (b) Breathing analysis depicting the accuracy of phase binning with the mean and standard deviation of tumor positions in each bin. There is minimal interbin crossover.

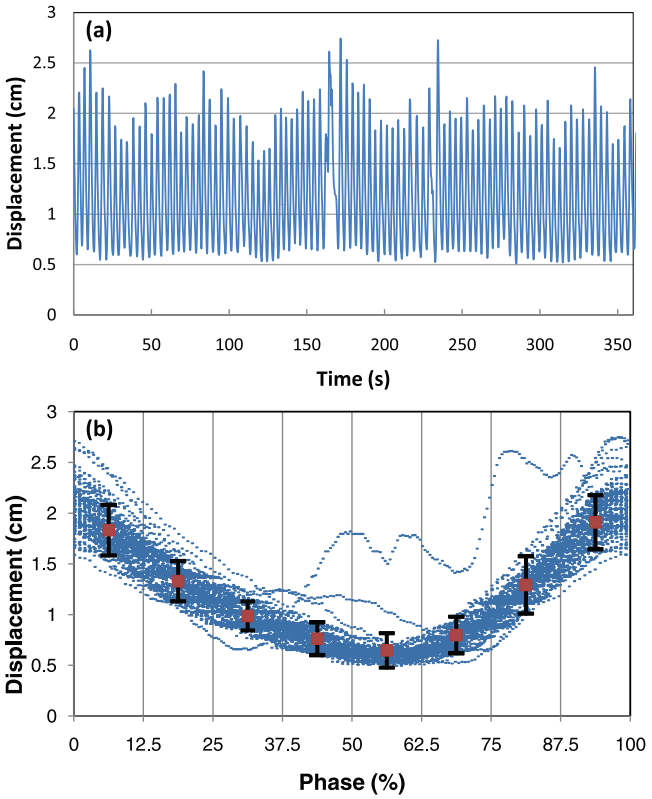

FIG. 3. (a) Phantom motion representing an average breather with some variation in breathing amplitude and period. (b) Breathing analysis depicting the accuracy of phase binning with the mean and standard deviation of tumor positions in each bin. There is some interbin crossover.

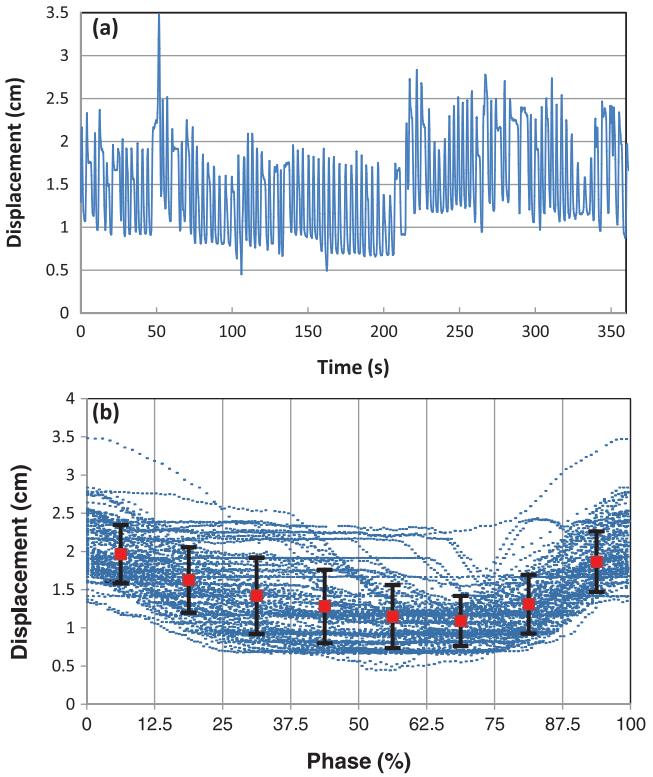

FIG. 4. (a) Phantom motion representing a patient with highly irregular breathing pattern. (b) Breathing analysis depicting the accuracy of phase binning with the mean and standard deviation of tumor positions in each bin. There is substantial interbin crossover.

separation and accuracy of the 4D PET data sorting between consecutive bins with almost zero overlap between adjacent phases. The peak inhale and exhale bins have the smallest standard deviations while intermediate bins have the largest. A more realistic breathing pattern has some variation in breathing amplitude [Fig. 3(a)] resulting in a phase sorted displacement graph that exhibits some degree of overlap between adjacent phases as well as phase errors [Fig. 3(b)]. If breathing is highly irregular [Fig. 4(a)], phase sorting error can result in poor separation between adjacent phases [Fig. 4(a)].

The 4D PET images using 4 and 8 gating bins for the 14 mm sphere are presented in Fig. 5. For both the ideal and average breather, 4D PET was able to reduce motion blurring thereby producing gated PET images which were closer in size to a static phantom effect. For highly irregular motion, the large phase binning error results in poorly separated PET bins with apparent tumor sizes larger than those of the ideal or average breather.

III.C. SUV measurements

4D PET SUV_{max} measurements were found to be systematically higher compared to the nongated PET SUV_{max} across all tumor sizes. For the ideal breather [Fig. 6(a)], the best bin (87%) had SUVs within (-5.4 ± 5.3)% of the static phantom measurements compared to (-18.4 ± 17.0)% for the worst (12%) bin and (-28.5 ± 18.2)% for the nongated scan when averaged over all tumor sizes. For the average breather [Fig. 6(b)], the best bin (37%) had SUVs within (-9.6 ± 13.0)% of the static phantom measurements compared to (-15.7 ± 12.6)% for the worst (62%) bin and (-25.9 ± 14.4)% for the nongated scan. For the highly irregular breather [Fig. 6(c)], the best bin (12%) had SUVs within (-17.1 ± 10.8)% of the static phantom measurements compared to (-25.4 ± 17.1)% for the worst (37%) bin and (-27.9 ± 18.2)% for the nongated scan. The 8 bin 4D PET measurements (Fig. 7) resulted in SUV_{max} that was on average larger than the 4 bin PET but with wider interbin variability. For the 14 mm sphere in the good breather, the 4 bin PET SUV_{max} was (11.5 ± 1.2) compared to (13.1 ± 1.9) for the 8 bin PET. Corresponding results for the average breather were (11.3 ± 0.4) for the 4 bin PET compared to (11.6 ± 1.3) for the 8 bin PET, and for the poor breather (9.7 ± 0.9) for the 4 bin PET compared to (10.3 ± 1.6) for the 8 bin PET. The same 4D PET results are also presented in Table I (4 bins) and Table II (8 bins).

IV. DISCUSSION

Achieving accurate and reliable quantification enhances the role of PET/CT in diagnosis and for assessing response to therapy. Motion is detrimental toward reaching this goal but is, in principle, correctable so that true lesion activity may be assessed. Results from computer simulations indicate that motion adversely impacts PET quantification when its

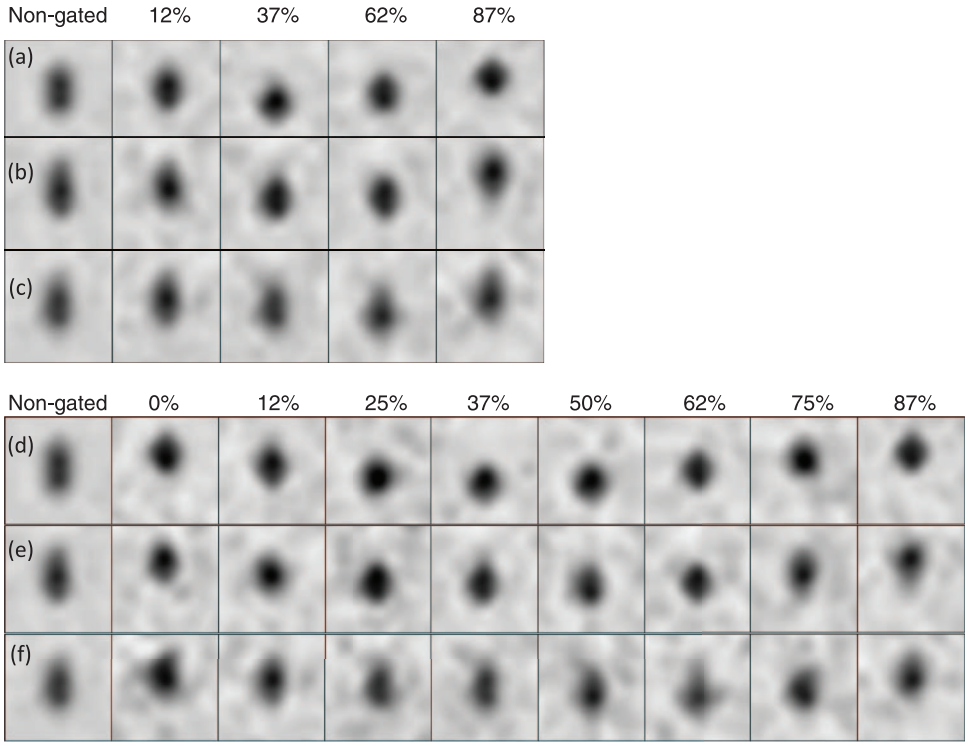

FIG. 5. Coronal 4D PET images using 4 gates for the ideal (a), average (b), and highly irregular breather (c) and using 8 gates for the ideal (d), average (e), and highly irregular breather (f).

amplitude is comparable to or greater than the size of the lesion. Since most respiratory related motion is less than 2 cm, the activity of small lesions is likely to be underestimated the most. Simulations indicate that motion blurring alone reduces the recovery coefficient by about 17% for a 15 mm tumor subject to 15 mm motion. The results presented in Fig. 1 facilitate the estimation of the impact of motion on tumor SUV for a range of lesion size and motion amplitude.

4D PET seeks to address respiratory motion blurring through the use of respiratory correlated data binning. Phase binning works well when breathing is highly regular, but amplitude and phase variations may result in binning error. Depending on the extent of breathing irregularities, 4D PET images with binning error are not completely motion free and exhibit some degree of residual blurring and interbin mixing. In practice, 4D PET SUVs lie somewhere between the "true"

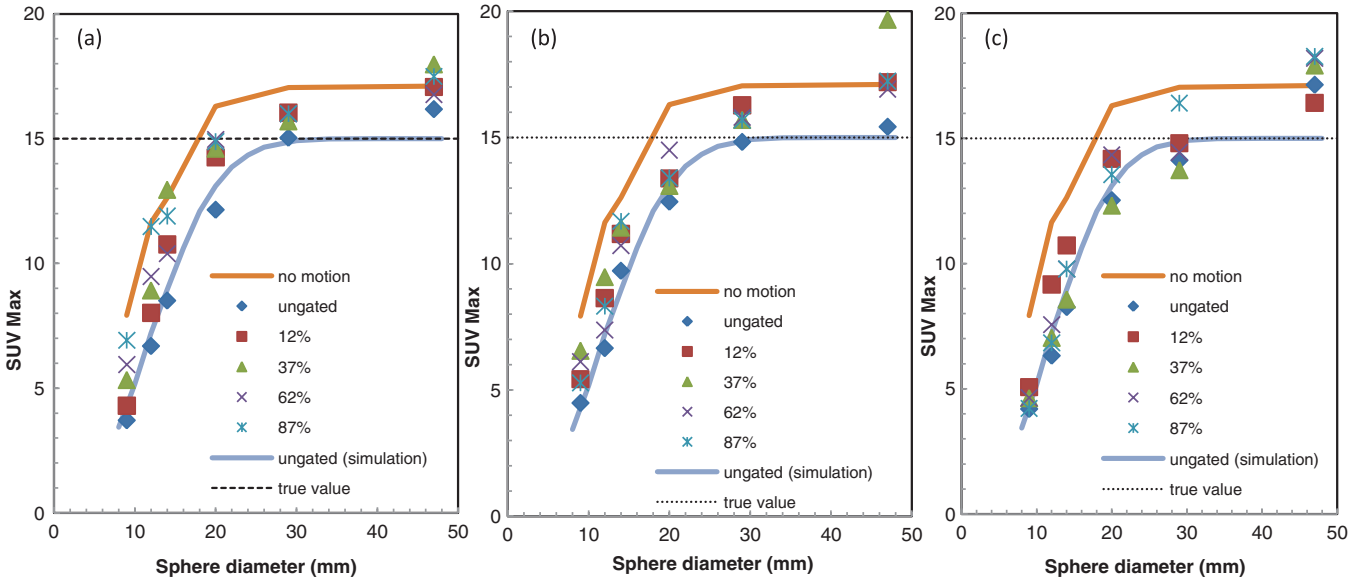

FIG. 6. 4D PET SUV_{max} using 4 bins for ideal (a), average (b), and highly irregular breather (c) compared to the nongated PET and no motion SUV_{max}. The phantom true SUV was 15.

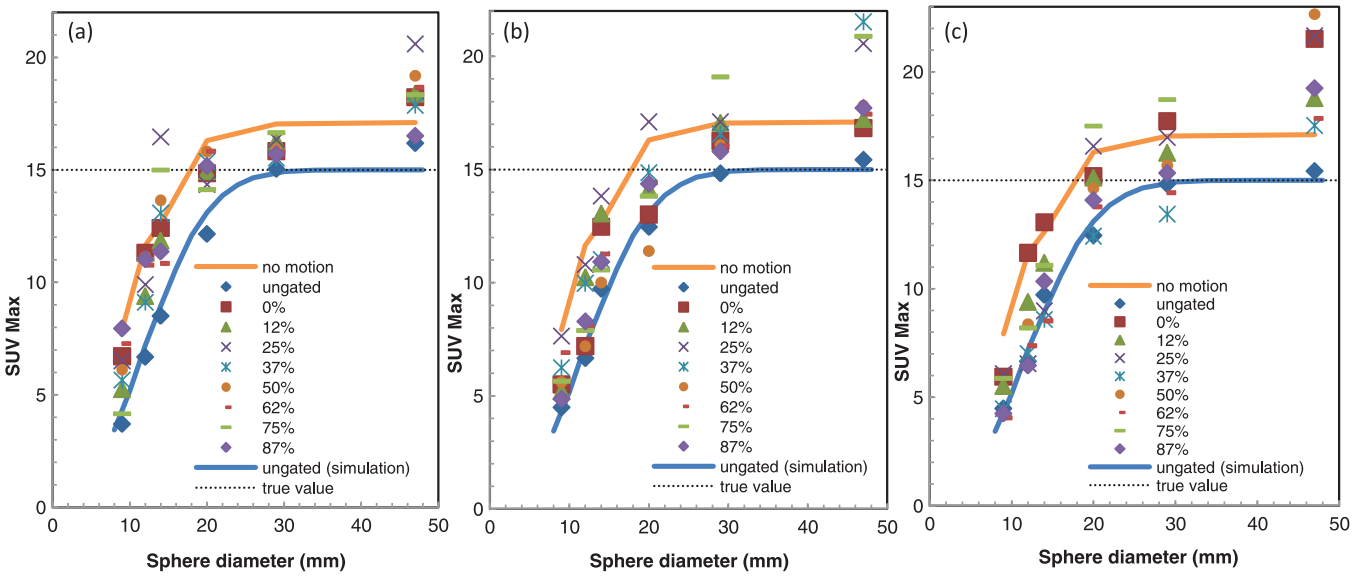

FIG. 7. 4D PET SUV_{max} using 8 bins for ideal (a), average (b), and highly irregular breather (c) compared to the nongated PET and no motion SUV_{max}. The phantom true SUV was 15.

(motion free) and nongated PET values. Nevertheless, even for a highly irregular breather, lesion motion can be visualized qualitatively using 4D PET as Fig. 5 depicts. As such, 4D PET SUVs should be used with caution as there is no simple means to assess the effects of breathing on the accuracy of data generated.

The pattern of human breathing [Fig. 3(a)] is aperiodic, exhibiting both breathing amplitude and rate variations from breathing cycle to breathing cycle. Breathing pattern variations lead to phase binning error and results in imperfect sorting of the PET data [Fig. 3(b)]. Phase binning error widens the range of tumor positions in individual bins even at peak inhale and exhale portions of the cycle, resulting in data mixing and bin overlap. In the case of a highly irregular breather [Fig. 4(a)], the bin overlap is comparable to the amplitude width in the bin [Fig. 4(b)]. Even though the average tumor position in the bins exhibits a cyclical motion, the individual PET bins are poorly sorted.

TABLE I. 4D PET SUVmax using 4 phase bins as a function of sphere diameter under different breathing conditions. The true SUVmax is 15.

	9 mm	12 mm	14 mm	20 mm	29 mm	47 mm
No motion	7.9	11.6	12.6	16.3	17.0	17.1
Regular ungated	3.7	6.7	8.5	12.2	15.0	16.2
Regular 12%	4.3	8.0	10.8	14.2	16.0	17.1
Regular 37%	5.3	8.9	13.0	14.6	15.7	18.0
Regular 62%	5.9	9.5	10.4	15.0	16.0	16.8
Regular 87%	6.9	11.5	11.9	14.9	16.0	17.5
Irregular ungated	4.5	6.7	9.7	12.5	14.8	15.4
Irregular 12%	5.4	8.6	11.2	13.4	16.3	17.2
Irregular 37%	6.6	9.5	11.4	13.1	15.7	19.7
Irregular 62%	6.1	7.4	10.7	14.5	15.8	16.9
Irregular 87%	5.3	8.3	11.7	13.4	15.7	17.2
Highly irregular ungated	4.2	6.3	8.3	12.5	14.1	17.1
Highly irregular 12%	5.1	9.2	10.7	14.2	14.8	16.4
Highly irregular 37%	4.6	7.0	8.6	12.3	13.7	17.9
Highly irregular 62%	4.6	7.6	9.8	14.3	14.4	18.2
Highly irregular 87%	4.2	6.8	9.8	13.6	16.4	18.3

TABLE II. 4D PET SUVmax using 8 phase bins as a function of sphere diameter under different breathing conditions. The true SUVmax is 15.

	9 mm	12 mm	14 mm	20 mm	29 mm	47 mm
No motion	7.9	11.6	12.6	16.3	17.0	17.1
Regular ungated	3.7	6.7	8.5	12.2	15.0	16.2
Regular 0%	6.7	11.3	12.4	14.8	15.8	18.2
Regular 12%	5.3	9.4	11.9	14.9	16.3	18.4
Regular 25%	6.5	9.9	16.5	14.3	16.3	20.6
Regular 37%	5.7	9.1	13.1	15.4	15.5	17.9
Regular 50%	6.1	11.1	13.7	15.8	15.9	19.2
Regular 62%	7.3	10.8	10.8	15.8	15.8	18.7
Regular 75%	4.2	11.0	15.0	14.1	16.6	18.3
Regular 87%	8.0	11.0	11.4	15.2	15.7	16.5
Irregular ungated	4.5	6.7	9.7	12.5	14.8	15.4
Irregular 0%	5.5	7.2	12.5	13.0	16.3	16.8
Irregular 12%	5.2	10.2	13.1	14.1	17.1	17.2
Irregular 25%	7.6	10.8	13.8	17.1	17.1	20.6
Irregular 37%	6.2	10.0	11.0	14.9	16.6	21.5
Irregular 50%	5.6	7.2	10.0	11.4	16.1	17.8
Irregular 62%	6.9	8.1	11.3	14.4	16.0	17.4
Irregular 75%	5.6	7.9	10.6	13.8	19.1	20.9
Irregular 87%	4.9	8.3	10.9	14.4	15.8	17.7
Highly irregular ungated	4.2	6.3	8.3	12.5	14.1	17.1
Highly irregular 0%	6.0	11.7	13.1	15.2	17.7	21.5
Highly irregular 12%	5.5	9.4	11.2	15.1	16.3	18.8
Highly irregular 25%	6.1	6.5	9.0	16.6	17.0	21.7
Highly irregular 37%	4.5	7.0	8.6	12.4	13.4	17.5
Highly irregular 50%	4.3	8.4	10.3	14.6	15.7	22.7
Highly irregular 62%	4.1	7.4	8.5	13.8	14.4	17.9
Highly irregular 75%	5.9	8.2	11.1	17.5	18.7	23.1
Highly irregular 87%	4.2	6.5	10.3	14.1	15.3	19.2

Other factors that affect the quantitative accuracy of 4D PET include attenuation correction errors, correlation of internal and external motion, and image noise. One problem relates to attenuation correction errors arising from the spatial mismatch between the PET and CT data.[10,14] These errors can impact clinical diagnosis and give rise to quantification errors, especially for lesions near the diaphragm where there is large heterogeneity in tissue attenuation and significant respiratory motion. Using a slow or averaged CT (Ref. 25) for attenuation correction has been suggested as a way to minimize these errors for nongated PET, while a phase matched 4D CT (Ref. 14) may be necessary for attenuation correction in a 4D PET protocol. In our study, the phantom was filled homogeneously with water (both for the lesions and background), and thus we were not able to simulate errors due to spatial mismatch of CT and PET as is the case for thoracic lesions in human studies. Inclusion of these errors is likely to further decrease the accuracy of quantitative gated 4D PET.

Respiratory signals derived from external body surrogates are assumed to have a direct correlation with internal respiratory motion. However, studies[26] have shown that the correlation using a single external landmark, as is used in the Varian RPM system, may be poor depending on tumor location. In the absence of real-time internal motion tracking such as from MRI, a multipoint binning approach using clustering[19] proposed in 4D CT imaging may potentially be translated for use in 4D PET. The choice of the number of 4D phase bins can affect the noise level and hence the SUV_{max}. Increasing the number of gates improves motion separation but biases tumor SUV_{max} upward[27] offsetting the drop in SUV arising from decreased motion blurring. This is evidenced by the larger interbin SUV standard deviations between the 4 bin and 8 bin PET results.

The results presented in this phantom study demonstrate the limitations of 4D PET under irregular motion. While only lesions with uniform activity concentration and a fixed tumor to background ratio could be simulated, the same adverse impact on SUV quantification would be expected in human studies but the effect of irregular breathing on 4D PET in lesions with inhomogeneous uptake is harder to quantify. The SUV_{max} was used to demonstrate the systematic decrease in quantitative accuracy as motion became more irregular. Other measures such as SUV_{mean} or partial volume corrected SUV, while not presented in this phantom study, are likely to show the same trend with motion irregularity as with the SUV_{max}.

While we have presented 4D PET results based only on the more widely available phase binning technique, it has been demonstrated that amplitude binning,[17,18] which is starting to be offered by commercial vendors, is the more accurate binning method. By its nature, amplitude binning will not exhibit the type of sorting errors arising from irregular breathing as depicted in Figs. 3 and 4 using the phase binning approach. An added advantage of amplitude binning is that the signal to noise can be improved through the addition of bins corresponding to the same amplitude but with opposing directions of motion.

The main application of 4D PET is in thoracic imaging, given the presence of respiratory motion. Since lesions located inferiorly in the thorax are more prone to motion than those located superiorly, the SUV measurements for these lesions are more likely to be underestimated owing to a combination of motion blurring and PVE. As the effect of motion and PVE reduce the measured SUV, both factors should be taken into account to achieve more quantitatively accurate SUVs. 4D PET alone can reduce the effect of motion blurring but PVE may still be the dominant source of quantitative inaccuracy for small lesions as shown in the simulation with a digital phantom. Motion blurring dominates only when the motion amplitude is comparable to the lesion size. Thus, the effect of motion blurring together with PVE is only likely to impact quantification of uptake in small lesions.

V. CONCLUSION

The quantitative accuracy of current 4D PET systems using phase binning can be affected by irregular breathing. Phase binning error decreases interbin motion separation and results in 4D SUVs that lie between the true (stationary) and nongated values. If the lesion is large compared to the amplitude of the motion, the impact on SUV will be small and 4D PET may not be necessary. 4D PET SUVs should not be taken at face value, and evaluation of the acquired respiratory signal may be required to ascertain the accuracy of SUVs obtained from 4D PET. In order to use 4D PET quantitatively, better data binning techniques have to be developed in order to decompose PET into multiple respiratory phases. The effect of partial volume error is most likely to dominate over motion effects for small lesions and both effects have to be considered in order to achieve quantitatively accurate SUVs.

ACKNOWLEDGMENTS

The authors thank Joel Karp for providing us technical insights and helpful suggestions. H.Z. is supported by the Swiss National Science Foundation under Grant No. SNSF 31003A-135576, Geneva Cancer League, the Indo-Swiss Joint Research Programme ISJRP 138866, and Geneva University Hospital under Grant No. PRD 11-II-1.

[a]Author to whom correspondence should be addressed. Electronic mail: teok@uphs.upenn.edu

[1]J. W. Fletcher, B. Djulbegovic, H. P. Soares, B. A. Siegel, V. J. Lowe, G. H. Lyman, R. E. Coleman, R. Wahl, J. C. Paschold, N. Avrill, L. H. Einhorn, W. W. Suh, D. Samson'O, D. Delbekell, M. Gorman, and A. F. Shields, "Recommendations on the Use of 18F-FDG PET in oncology," J. Nucl. Med. **49**(3), 480–508 (2008).

[2]T. C. Kwee, S. Basu, B. Saboury, A. Alavi, and D. A. Torigian, "Functional oncoimaging techniques with potential clinical applications," Front. Biosci. **E4**(3), 1081–1096 (2012).

[3]K. Mah, C. B. Caldwell, Y. C. Ung, C. E. Danjoux, J. M. Balogh, S. N. Ganguli, L. E. Ehrlich, and R. Tirona, "The impact of 18FDG-PET on target and critical organs in CT-based treatment planning of patients with poorly defined non-small-cell lung carcinoma: A prospective study," Int. J. Radiat. Oncol., Biol., Phys. **52**(2), 339–350 (2002).

[4]K. J. Biehl, F. M. Kong, F. Dehdashti, J. Y. Jin, S. Mutic, I. El Naqa, B. A. Siegel, and J. D. Bradley, "F-18-FDG PET definition of gross tumor volume for radiotherapy of non-small cell lung cancer: Is a single

standardized uptake value threshold approach appropriate?," J. Nucl. Med. **47**(11), 1808–1812 (2006).
[5]E. G. Troost, D. A. Schinagl, J. Bussink, W. J. Oyen, and J. H. Kaanders, "Clinical evidence on PET-CT for radiation therapy planning in head and neck tumours," Radiother. Oncol. **96**(3), 328–334 (2010).
[6]C. T. Muijs, J. C. Beukema, J. Pruim, V. E. Mul, H. Groen, J. T. Plukker, and J. A. Langendijk, "A systematic review on the role of FDG PET/CT in tumour delineation and radiotherapy planning in patients with esophageal cancer," Radiother. Oncol. **97**(2), 165–171 (2010).
[7]M. Mac Manus and R. J. Hicks, "The use of positron emission tomography(PET) in the staging/evaluation, treatment, and follow-up of patients with lung cancer: A critical review," Int. J. Radiat. Oncol., Biol., Phys. **72**(5), 1298–1306 (2008).
[8]G. J. Kubicek and D. E. Heron, "Clinical applications of PET-computed tomography in planning radiotherapy: General principles and an overview," PET Clinics **6**(2), 105–115 (2011).
[9]H. Zaidi and I. El Naqa, "PET-guided delineation of radiation therapy treatment volumes: A survey of image segmentation techniques," Eur. J. Nucl. Med. Mol. Imaging. **37**(11), 2165–2187 (2010).
[10]M. M. Osman, C. Cohade, Y. Nakamoto, and R. L. Wahl, "Respiratory motion artifacts on PET emission images obtained using CT attenuation correction on PET-CT," Eur. J. Nucl. Med. Mol. Imaging **30**(4), 603–606 (2003).
[11]Y. E. Erdi, S. A. Nehmeh, T. Pan, A. Pevsner, K. E. Rosenzweig, G. Mageras, E. D. Yorke, H. Schoder, W. Hsiao, O. D. Squire, P. Vernon, J. B. Ashman, H. Mostafavi, S. M. Larson, and J. L. Humm, "The CT motion quantitation of lung lesions and its impact on PET-measured SUVs," J. Nucl. Med. **45**(8), 1287–1292 (2004).
[12]S. A. Nehmeh, Y. E. Erdi, C. C. Ling, K. E. Rosenzweig, H. Schoder, S. M. Larson, H. A. Macapinlac, O. D. Squire, and J. L. Humm, "Effect of respiratory gating on quantifying PET images of lung cancer," J. Nucl. Med. **43**(7), 876–881 (2002).
[13]S. A. Nehmeh and Y. E. Erdi, "Respiratory motion in positron emission tomography/computed tomography: A review," Semin. Nucl. Med. **38**(3), 167–176 (2008).
[14]S. A. Nehmeh, Y. E. Erdi, T. Pan, A. Pevsner, K. E. Rosenzweig, E. Yorke, G. S. Mageras, H. Schoder, P. Vernon, O. Squire, H. Mostafavi, S. M. Larson, and J. L. Humm, "Four-dimensional (4D) PET/CT imaging of the thorax," Med. Phys. **31**(12), 3179–3186 (2004).
[15]S. A. Nehmeh, Y. E. Erdi, G. S. P. Meirelles, O. Squire, S. M. Larson, J. L. Humm, and H. Schoder, "Deep-inspiration breath-hold PET/CT of the thorax," J. Nucl. Med. **48**(1), 22–26 (2007).
[16]S. A. Nehmeh, Y. E. Erdi, C. C. Ling, K. E. Rosenzweig, O. D. Squire, L. E. Braban, E. Ford, K. Sidhu, G. S. Mageras, S. M. Larson, and J. L. Humm, "Effect of respiratory gating on reducing lung motion artifacts in PET imaging of lung cancer," Med. Phys. **29**(3), 366–337 (2002).
[17]M. Dawood, F. Buther, N. Lang, O. Schober, and K. P. Schafers, "Respiratory gating in positron emission tomography: A quantitative comparison of different gating schemes," Med. Phys. **34**(7), 3067–3076 (2007).
[18]G. Chang, T. Chang, T. Pan, J. W. Clark, and O. R. Mawlawi, "Implementation of an automated respiratory amplitude gating technique for PET/CT: Clinical evaluation," J. Nucl. Med. **51**(1), 16–24 (2010).
[19]C. Gianoli, M. Riboldi, M. F. Spadea, L. L. Travaini, M. Ferrari, R. Mei, R. Orecchia, and G. Baroni, "A multiple points method for 4D CT image sorting," Med. Phys. **38**(2), 656–667 (2011).
[20]M. Soret, S. L. Bacharach, and I. Buvat, "Partial-volume effect in PET tumor imaging," J. Nucl. Med. **48**(6), 932–945 (2007).
[21]L. Geworski, B. O. Knoop, M. L. de Cabrejas, W. H. Knapp, and D. L. Munz, "Recovery correction for quantitation in emission tomography: A feasibility study," Eur. J. Nucl. Med. **27**(2), 161–169 (2000).
[22]K. Baete, J. Nuyts, K. Van Laere, W. Van Paesschen, S. Ceyssens, L. De Ceuninck, O. Gheysens, A. Kelles, J. Van den Eynden, P. Suetens, and P. Dupont, "Evaluation of anatomy based reconstruction for partial volume correction in brain FDG-PET," Neuroimage **23**(1), 305–317 (2004).
[23]B. K. Teo, Y. Seo, S. L. Bacharach, J. A. Carrasquillo, S. K. Libutti, H. Shukla, B. H. Hasegawa, R. A. Hawkins, and B. L. Franc, "Partial-volume correction in PET: Validation of an iterative postreconstruction method with phantom and patient data," J. Nucl. Med. **48**(5), 802–810 (2007).
[24]I. El Naqa, D. A. Low, J. D. Bradley, M. Vicic, and J. O. Deasy, "Deblurring of breathing motion artifacts in thoracic PET images by deconvolution methods," Med. Phys. **33**(10), 3587–3600 (2006).
[25]T. Pan, O. Mawlawi, S. A. Nehmeh, Y. E. Erdi, D. Luo, H. H. Liu, R. Castillo, R. Mohan, Z. Liao, and H. A. Macapinlac, "Attenuation correction of PET images with respiration-averaged CT images in PET/CT," J. Nucl. Med. **46**(9), 1481–1487 (2005).
[26]N. Koch, H. H. Liu, G. Starkschall, M. Jacobson, K. Forster, Z. Liao, R. Komaki, and C. W. Stevens, "Evaluation of internal lung motion for respiratory-gated radiotherapy using MRI: Part I—Correlating internal lung motion with skin fiducial motion," Int. J. Radiat. Oncol., Biol., Phys. **60**, 1459–1472 (2004).
[27]C. Liu, A. Alessio, L. Pierce, K. Thielemans, S. Wollenweber, A. Ganin, and P. Kinahan, "Quiescent period respiratory gating for PET/CT," Med. Phys. **37**(9), 5037–5043 (2010).